Supplementary information for

(3+2)D Modulation Governs Vacancy Ordering and Oxide-Ion Transport in γ-Type BIMEVOX conductors

Yajun Yue[a, b, c], Fengjin Qu[a,c*], Aleksandra Dzięgielewska[d], Anucha Koedtruad[a,c], Qifeng Zheng[b], Wang Hay Kan[a, c], Stephen Hull[e], Marcin Malys[d], Marcin Krynski[d], Franciszek Krok[d], Takashi Honda[f], Shuki Torii[f], Vaclav Petricek[g*], Isaac Abrahams[h*], and Ping Miao[a,c*]

[a]Spallation Neutron Source Science Center, China Spallation Neutron Source, Dongguan, Guangdong, 523803, China.

[b]School of Chemistry, South China Normal University, Guangzhou 510006, Guangdong, China.

[c]Institute of High Energy Physics Chinese Academy of Sciences, Beijing, 100049, People's Republic of China.

[d]Faculty of Physics, Warsaw University of Technology, ul. Koszykowa 75, 00-662 Warsaw, Poland.

[e]Science and Technology Facilities Council, ISIS Facility, Rutherford Appleton Laboratory, Chilton, Didcot, Oxon. OX11 OQX, U.K.

[f]Institute of Materials Structure Science, High Energy Accelerator Research Organization (KEK), Tsukuba, Ibaraki 305-0801, Japan.

[g]Department of Structure Analysis, Institute of Physics of the Czech Academy of Sciences, Na Slovance 2, 182 00 Prague 8, Czech Republic.

[h]Department of Chemistry, Queen Mary University of London, Mile End Road London, E1 4NS, U.K.

***Corresponding Authors**

Fengjin Qu

Email: qufj@ihep.ac.cn

Vaclav Petricek

Email: petricek@fzu.cz

Isaac Abrahams

Email: i.abrahams@qmul.ac.uk

Ping Miao

Email: miaoping@ihep.ac.cn

Contents

Figures 3

Fig. S1 3

Fig. S2 3

Fig. S3 4

Fig. S4 4

Fig. S5 5

Fig. S6 6

Fig. S7 6

Fig. S8 7

Fig. S9 7

Tables 8

Table. S1 8

Table. S2 8

Table. S3 8

Table. S4 9

Table. S5 10

Table. S6 10

Table. S7 11

Table. S8 11

Figures

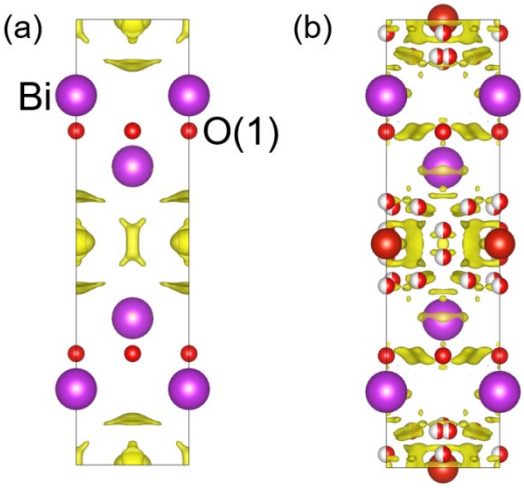

Fig. S1 Difference Fourier maps for BICUVOX.10 at room temperature, showing diffuse electron density (a) before and (b) after assigning atoms in the vanadate layer.

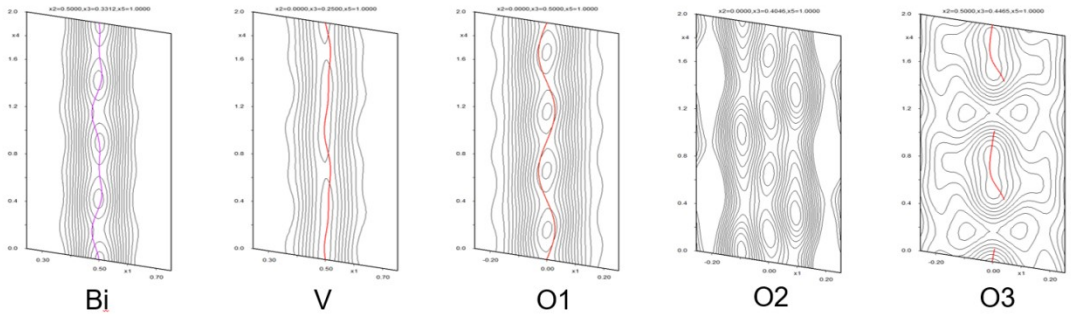

Fig. S2 F_{obs} de Wolff sections for γ′-BICUVOX.10, showing electron densities of atoms in the x_1–x_4 plane. Coloured lines indicate positional modulation functions.

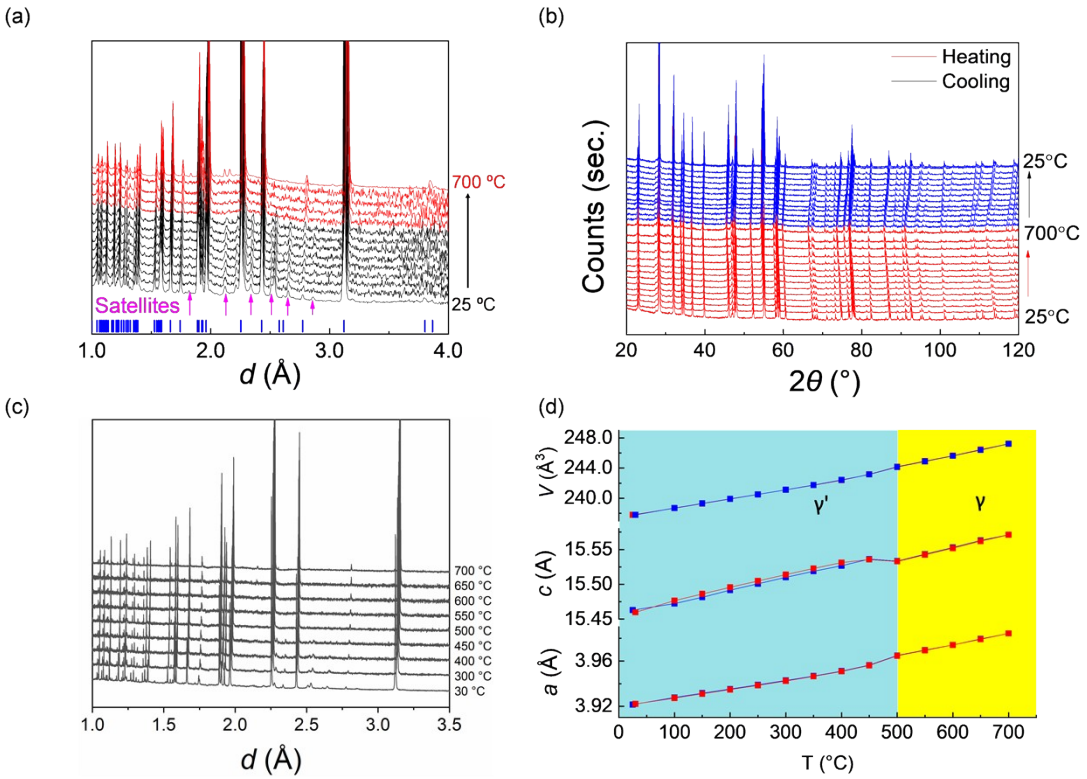

Fig. S3 (a) Neutron powder diffraction patterns (bank 4) collected during heating from 25 to 700 °C. (b) Powder XRD patterns for BICUVOX.10 on heating and cooling. (c) High-resolution neutron powder diffraction patterns of BICUVOX.10 on heating collected on Super-HRPD at JPARC and (d) thermal variation of refined tetragonal (sub)cell lattice parameters and volume on heating (red) and cooling (blue).

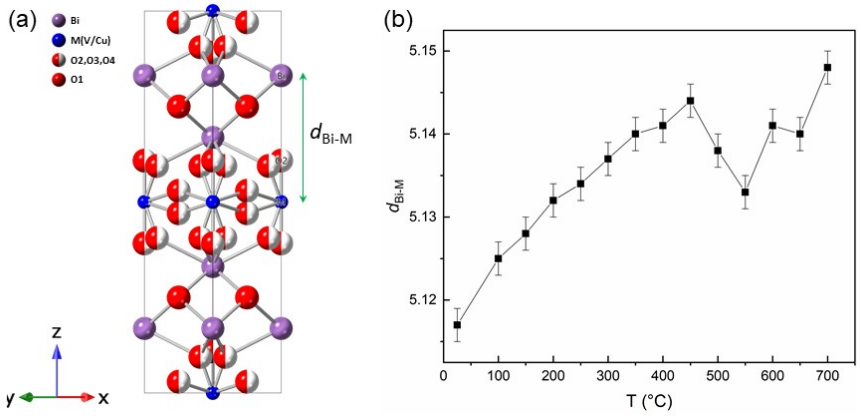

Fig. S4 (a) Projection showing interlayer Bi-M (M = V/Cu) distance, d_{Bi-M} in the average structure of BICUVOX.10 and (b) thermal variation of d_{Bi-M}.

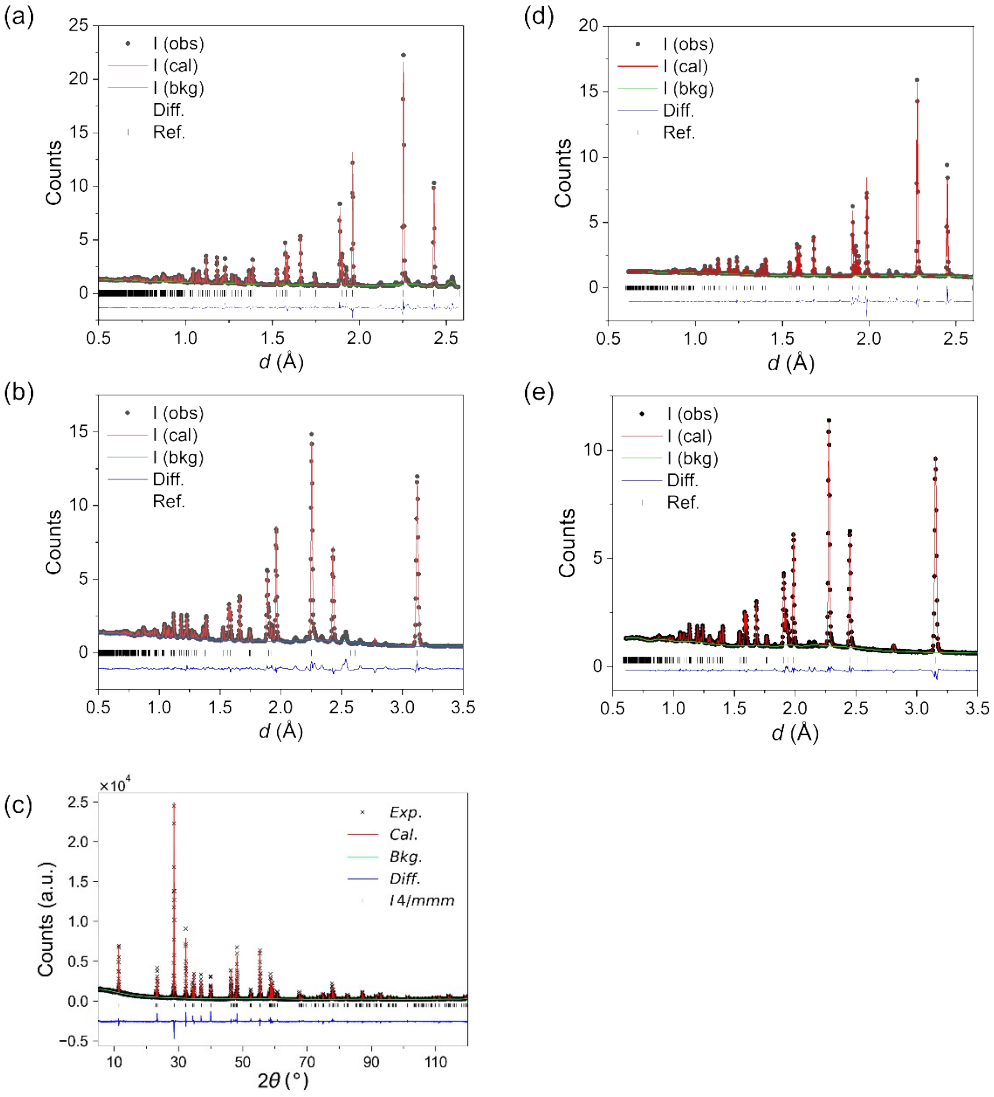

Fig. S5 Fitted neutron diffraction patterns for BICUVOX.10 at (a-c) 25 °C and (d-e) 700 °C showing fits to (a, d) neutron back scattering, (b, e) neutron 90° and (c) X-ray data.

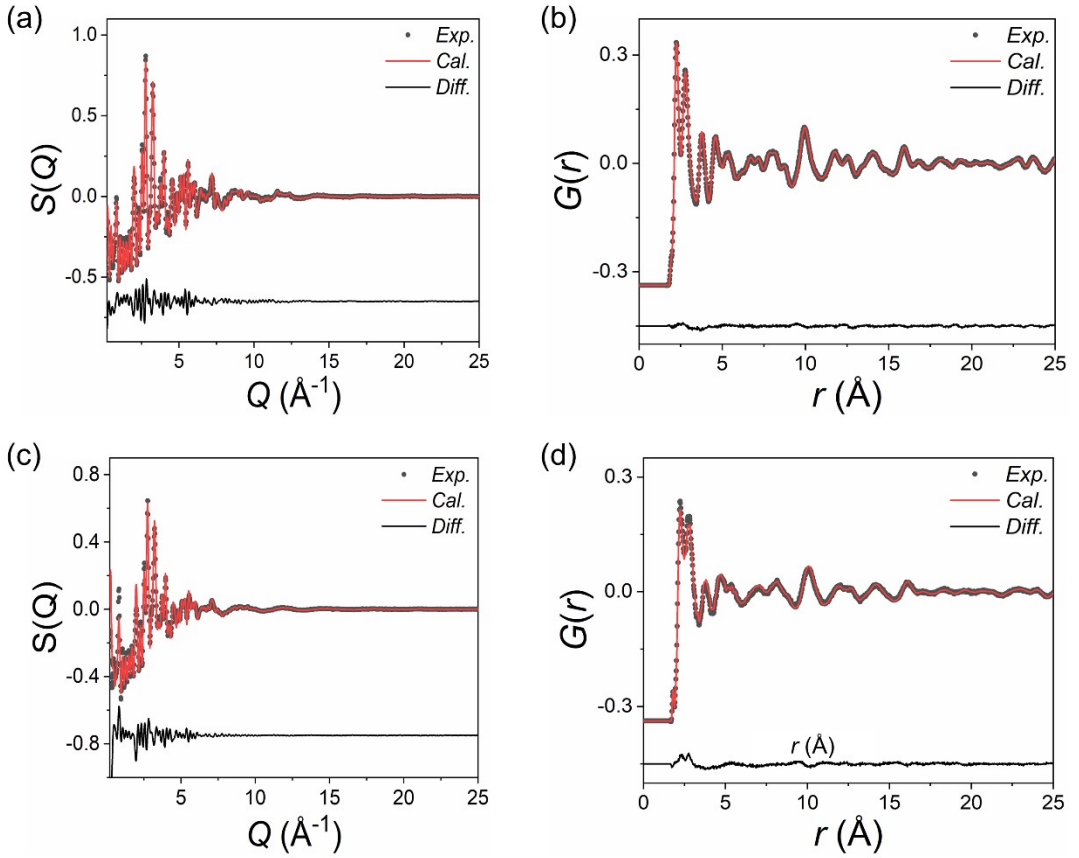

Fig. S6 Fitted (a,c) $S(Q)$ and (b,d) $G(r)$ profiles at (a,b) 25 °C, and (c,d) 700 °C for BICUVOX.10.

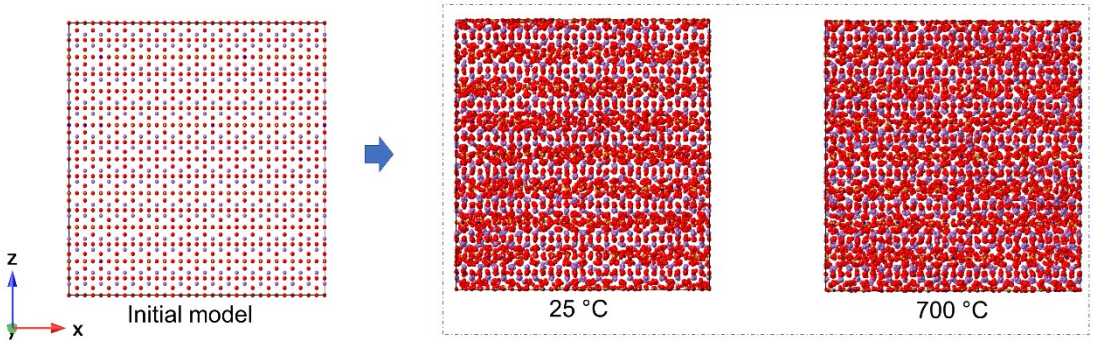

Fig. S7 Representative initial and final RMC models for BICUVOX.10.

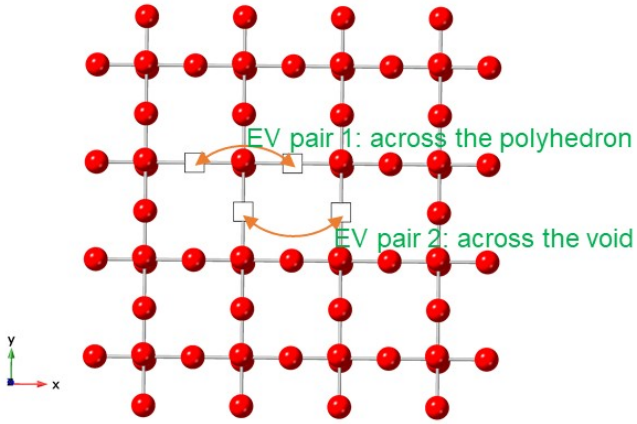

Fig. S8 Schematic diagram showing the relative locations of next nearest neighbour equatorial vacancy pairs in the vanadate layer of BICUVOX.10.

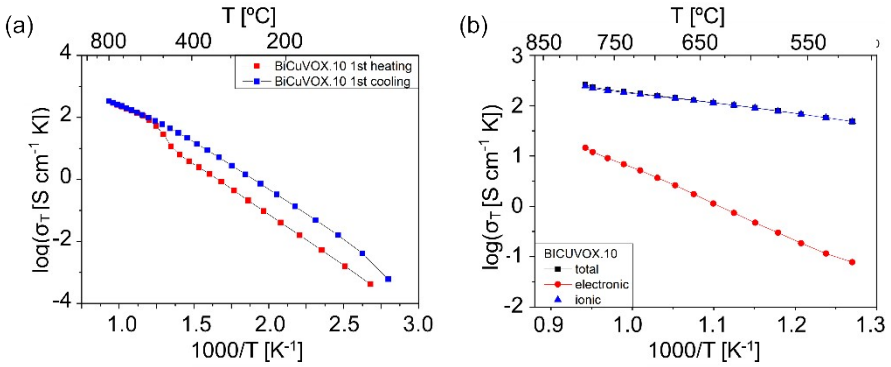

Fig. S9 (a) Arrhenius plots of total conductivity for BICUVOX.10 during the first heating and cooling cycle, (b) ionic and electronic conductivity contributions to total conductivity (cooling data).

Tables

Table. S1 Crystal and refinement parameters for the modulated γ′-phase of BICUVOX.10 from single crystal X-ray diffraction. Estimated standard deviations are given in parentheses.

Chemical formula	$Bi_2V_{0.9}Cu_{0.1}O_{5.35}$
Superspace group	*I*4/*mmm*(a,a,1)0s0s(-a,a,1)0s00
Temperature (K)	100
Lattice parameters (Å)	*a* = 3.9237(2) *c* = 15.4019(7)
Volume (Å^3)	237.12(2)
Z	2
Density (calc) g cm^{-3}	7.8467
F(000)	469
Radiation	Mo *K*α
Parameters/constraints	134/27
Weighting scheme	$w = 1/[(\sigma^2(F_o^2)+(0.094474P)^2]$, where $P = (F_o^2+2F_c^2)/3$
Total reflections collected	1874 = 1277+597
R_w	0.2005
GOF(all data)	1.54

Table. S2 Refined atomic parameters for γ′-phase BICUVOX.10 in the average structure model (space group *I*4/*mmm*) at 100 K, from single crystal X-ray diffraction data. Estimated standard deviations are given in parentheses.

Atom	Site	*x*	*y*	*z*	Occ.	U_{11} (Å^2)	U_{22} (Å^2)	U_{33} (Å^2)
Bi	4*e*	0.0	0.0	0.1688(1)	1.0	0.0357(6)	0.0357(6)	0.0218(7)
V/Cu	2*b*	0.5	0.5	0.0	0.9/0.1	0.051(3)	0.051(3)	0.007(2)
O(1)	4*d*	0.0	0.5	0.25	1.0	0.016(3)	0.016(3)	0.040(6)
O(2)	4*e*	0.5	0.5	0.095(2)	0.5	0.10(1)	0.10(1)	0.03(1)
O(3)	8*g*	0.5	0.0	0.055(3)	0.5875	0.06(1)	0.12(2)	0.09(1)

Table. S3 Site occupancies atomic displacement parameter (ADP) type and modulation functions for γ′-BICUVOX.10.

Atom	Occ.	ADP type	Positional modulation	Occupational modulation	ADP modulation
Bi	1	Anharmonic	10	0	20
V	0.9	Anharmonic	10	10	20
Cu	0.1	Anharmonic	10	10	20
O(1)	1	Harmonic	0	10	0
O(2)	0.5875	Harmonic	10	10	0
O(3)	0.5	Harmonic	10	10	0

Table. S4 Crystal and refinement parameters for BICUVOX.10 at 25 °C and 700 °C using the *I*4/*mmm* model from a combined analysis of powder X-ray and neutron diffraction data. The neutron diffraction data were from the Polaris instrument at ISIS. Estimated standard deviations are given in parentheses.

Sample Name		BICUVOX10	
Chemical formula		$Bi_2V_{0.9}Cu_{0.1}O_{5.35}$	
Temperature (°C)		25 °C	700 °C
Crystal system		*I*4/*mmm*	*I*4/*mmm*
Lattice parameters (Å)	*a*	3.92028(9)	3.9692(1)
	c	15.4550(4)	15.5484(5)
Volume (Å^3)		237.52(2)	244.96(2)
Z		2	2
Density (calc) g cm^{-3}		7.771	7.535
R-factors	Neutron back scattering	R_{wp} = 0.0224 R_p = 0.0406 R_{ex} = 0.0032 R_{F^2} = 0.2089	R_{wp} = 0.0158 R_p = 0.0257 R_{ex} = 0.0031 R_{F^2} = 0.0996
	Neutron 90°	R_{wp} = 0.0284 R_p = 0.0434 R_{ex} = 0.0031 R_F^2 = 0.2998	R_{wp} = 0.0143 R_p = 0.0192 R_{ex} = 0.0031 R_{F^2} = 0.0696
	X-ray	R_{wp} = 0.0913 R_p = 0.0675 R_{ex} = 0.0462 R_F^2 = 0.1410	
	Totals	R_{wp} = 0.0191 R_p = 0.0889	R_{wp} = 0.0149 R_p = 0.0224
No. of variables		119	101
χ^2		31.11	18.23
No. of profile points	Neut. (bs) (90 °C) X-ray	1917 2788 6879	1446 1771

Table. S5 Refined atomic parameters for BICUVOX.10 at 25 °C and 700 °C using the *I*4/*mmm* model from a combined analysis of powder X-ray and neutron diffraction data. The neutron diffraction data were from the Polaris instrument. Estimated standard deviations are given in parentheses.

25 ˚C						
Atom	Site	*x*	*y*	*z*	Occ.	U_{iso} (Å^2)
Bi	4*e*	0.0	0.0	0.16898(4)	1.0	0.0209(3)
M (V/Cu)	2*b*	0.5	0.5	0.0	0.9/0.1	0.012(3)
O(1)	4*d*	0.0	0.5	0.25	1.0	0.0205(3)
O(2)	4*e*	0.5	0.5	0.1082(4)	0.236(9)	0.0394(2)
O(3)	8*g*	0.5	0.0	0.0299(2)	0.3375	0.0699(9)
O(4)	16*n*	0.5	0.0316(2)	0.0944(3)	0.191(2)	0.064(1)
700 ˚C						
Atom	Site	*x*	*y*	*z*	Occ.	U_{iso} (Å^2)
Bi	4e	0.0	0.0	0.16939(6)	1.0	0.0525(8)
M (V/Cu)	2b	0.5	0.5	0.0	0.9/0.1	0.02
O(1)	4d	0.0	0.5	0.25	1.0	0.0460(7)
O(2)	4e	0.5	0.5	0.1070(5)	0.36(2)	0.070(4)
O(3)	8g	0.5	0.0	0.0271(3)	0.3375	0.129(2)
O(4)	16n	0.5	0.297(3)	0.0883(4)	0.160(5)	0.068(2)

Table. S6 Significant contact distances in BICUVOX.10 at 25 °C and 700 °C using the *I*4/*mmm* model from a combined analysis of powder X-ray and neutron diffraction data. The neutron diffraction data were from the Polaris instrument. Estimated standard deviations are given in parentheses.

Temp.	Bond	Distance (Å)	Bond	Distance (Å)
25 °C	Bi-O(1)	2.3317 (1)	V/Cu-O(2)	1.643(2)
	Bi-O(4)	2.569(1)	V/Cu-O(3)	2.0207(2)
			V/Cu-O(4)	1.625(2)
700 °C	Bi-O(1)	2.3472(5)	V/Cu-O(2)	1.663(8)
	Bi-O(4)	2.630(5)	V/Cu-O(3)	2.029(1)
			V/Cu-O(4)	1.592(6)

Table. S7 Mean and mode contact distances for Bi–O, M–O, and O–O correlations from RMC analysis of neutron total scattering data (from Polaris) for BICUVOX.10 at 25 °C and 700 °C. Standard deviations from 10 parallel configurations are given in parentheses.

Temperature	Type	Mean dist. (Å)	Mode dist. (Å)
25 °C	Bi-O	2.318(2)	2.241(2)
	V-O	1.917(1)	1.853(1)
	Cu-O	1.933(2)	1.861(8)
	O-O	2.904(3)	2.740(3)
700 °C	Bi-O	2.334(2)	2.210(2)
	V-O	1.919(1)	1.853(1)
	Cu-O	1.891(4)	1.813(9)
	O-O	2.908(2)	2.725(2)

Table. S8 Equatorial and apical oxygen atom/oxygen vacancy total and percentage site occupancies in RMC models of BICUVOX.10 at 25 and 700 ºC. Standard deviations from 10 parallel configurations are given in parentheses.

	Apical O	Equatorial O	Apical vacancy	Equatorial vacancy
25 ºC				
Average Occ.	3742(10)	3119(10)	354(10)	977(10)
Percentage (%)	91.4(2)	76.1(2)	8.6(2)	23.9(2)
700 ºC				
Average Occ.	3935(5)	2926(5)	161(5)	1170(5)
Percentage (%)	96.1(1)	71.4(1)	3.9(1)	28.6(1)